SCIENTIFIC REPORTS

OPEN

SUBJECT AREAS:
MAGNETIC PROPERTIES AND MATERIALS
ELECTRONIC STRUCTURE

Received
30 January 2014

Accepted
21 March 2014

Published
9 April 2014

Correspondence and requests for materials should be addressed to H.W. (wuh@fudan.edu.cn)

Impact of spin-orbit coupling on the magnetism of Sr_3MIrO_6 (M = Ni, Co)

Xuedong Ou & Hua Wu

Laboratory for Computational Physical Sciences (MOE), State Key Laboratory of Surface Physics, and Department of Physics, Fudan University, Shanghai 200433, China.

Iridates are of current great interest for their entangled spin-orbital state and possibly exotic properties. In this work, using density functional calculations, we have demonstrated that the hexagonal spin-chain materials Sr_3MIrO_6 (M = Ni, Co) are an iridate system in which the spin-orbit coupling (SOC) tunes the magnetic and electronic properties. The significant SOC alters the orbital state, the exchange pathway, and thus the magnetic structure. This work clarifies the nature and the origin of the intra-chain antiferromagnetism of Sr_3MIrO_6 and well accounts for the most recent experiments.

Charge, spin and orbital states are often coupled in 3d transition-metal oxides due to their multiple degrees of freedom and electron correlation. These states are closely related to diverse material properties and functionalities, e.g., charge ordering, orbital ordering, spin-state and magnetic transition, metal-insulator transition, superconductivity, colossal magnetoresistance, and multiferroicity. It is therefore very important to study those charge-spin-orbital states and their fascinating coupling for modeling and understanding of the abundant properties. This has formed a research stream in condensed matter physics over past decades, see e.g., a short review by Dagotto[1]. Very recently, research interest has been extended to 5d transition-metal oxides, which probably possess a significant spin-orbit coupling and provide an avenue to novel magnetic and electronic properties due to an entangled spin-orbital state.

In this respect, iridates are a representative example[2–17]. An octahedrally coordinated iridium ion normally has a large t_{2g}-e_g crystal-field splitting due to the delocalized character of its 5d electrons. The resultant low-spin state with only a t_{2g} occupation makes an open shell Ir^{n+} ion (e.g., t_{2g}^5 for n = 4) behave effectively like p electrons (with an effective orbital momentum $\tilde{l}=1$). As a result, an intrinsic strong spin-orbit coupling (SOC) splits the t_{2g} levels into a lower $\tilde{j}=3/2$ quartet and a higher $\tilde{j}=1/2$ doublet. Then, for an Ir^{4+} constituent oxide, the half-filled $\tilde{j}=1/2$ doublet may form, due to a moderate electron correlation, a novel $\tilde{j}=1/2$ Mott insulating state[2,3]. It has been proposed that such a spin-orbital entangled state can bring about exotic properties, e.g., correlated topological insulator[4,5], superconductivity[6], Kitaev model[7,8], Weyl semimetal[9], and unusual magnetism[10].

In this Report, we have studied the 3d–5d transition-metal hybrid material Sr_3MIrO_6 (M = Ni, Co), and find that the SOC has a significant impact on its magnetism by tuning its spin-orbital states and the Ir-M inter-orbital interactions. This system has a general chemical formula $A_3MM'O_6$ (A = Ca, Sr; M = 3d transition metal, M' = 3d, 4d, 5d transition metal) and displays an in-plane hexagonal structure and out-of-plane spin chains, see Fig. 1. Those quasi one-dimensional spin chains each consist of alternating face-sharing MO_6 trigonal prisms and $M'O_6$ octahedra. This system drew a lot of attention in the past decade[18–27], because of its intriguing step-wise magnetization, significant Ising-like magnetism, thermoelectricity, and multiferroicity. Sr_3NiIrO_6 and Sr_3CoIrO_6 also possess fascinating magnetism[28–31]. Owing to their complex temperature-dependent magnetic transitions, a standing issue is the nature of their dominant intrachain magnetism: either an intrachain ferromagnetic (FM) exchange[28,29] or an antiferromagnetic (AF) coupling[30,31] was proposed in previous studies. Moreover, the origin of the magnetism remains elusive. Therefore, Sr_3NiIrO_6 and Sr_3CoIrO_6 call for a prompt study to clarify the nature and origin of their intriguing intrachain magnetism. As seen below, we make a comparative study for Sr_3NiIrO_6 and Sr_3CoIrO_6, by carrying out a systematic set of electronic structure calculations. Our results consistently explain the experimental observations and settle the standing issue. In particular, we find that the SOC of the Ir^{4+} ion plays an essential role in determining the intrachain AF structure of Sr_3MIrO_6 (M = Ni, Co) by tuning the crystal-field level sequence and altering the Ir-M inter-orbital interactions. Therefore, Sr_3MIrO_6 is added to the iridate category which highlights the significance of the SOC.

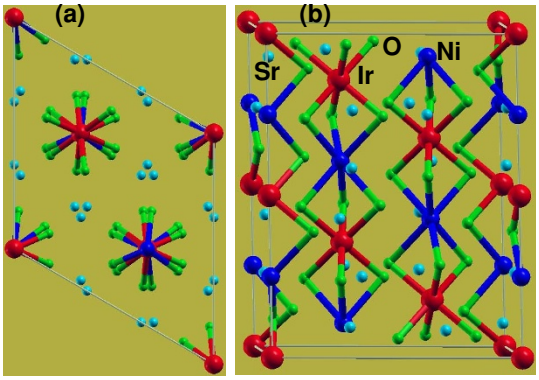

Figure 1 | Crystal structure plot of Sr_3MIrO_6 (a) projected onto the ab plane and (b) in a perspective view. It has a hexagonal ab plane and quasi one-dimensional $MIrO_6$ spin chains extending along the c-axis, in which the IrO_6 octahedra and MO_6 trigonal prisms are alternating.

Results

Crystal-field levels. We first carry out spin-restricted LDA calculations to estimate the crystal field splitting. The calculated DOS (density of states) results for Sr_3NiIrO_6 are shown in Fig. 2. The O 2p valence bands lie in between −7 and −2 eV. They have a significant covalency with the delocalized Ir 5d orbital and bring about the Ir 5d bonding state around −6 eV. A relatively weak Ni-O hybridization yields the Ni 3d bonding state in between −2 and −4 eV. Both the Ir 5d and Ni 3d antibonding states lie above −2 eV. For the Ir ion, its local octahedral coordination but a trigonal crystal field in the global coordinate system split the otherwise t_{2g} triplet into the e'_g doublet and the a_{1g} singlet both of the concern. The e_g doublet is far above them by 3 eV and is out of the concern. The a_{1g} singlet can be written as $3z^2 - r^2$, as the z-axis of the hexagonal lattice is

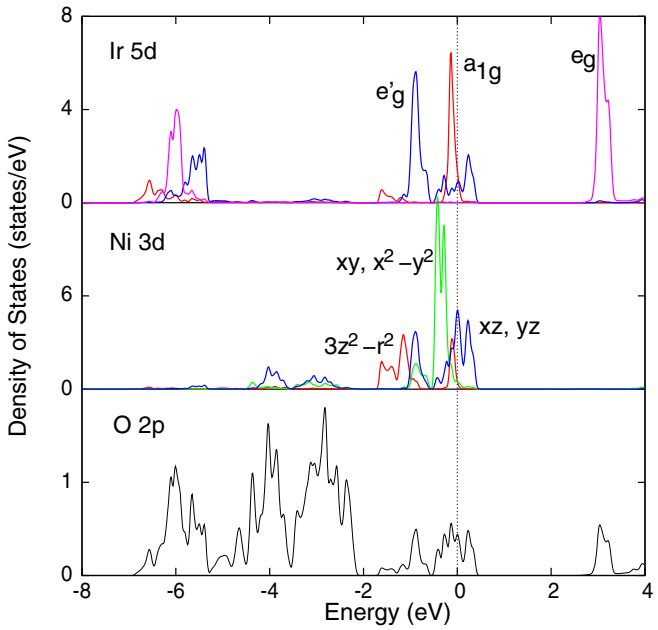

Figure 2 | Partial density of states (DOS) of Sr_3NiIrO_6 in the nonmagnetic state calculated by LDA. The octahedral Ir ion has a common large $t_{2g} - e_g$ crystal field splitting of more than 3 eV; and in a trigonal crystal field (elongation of the IrO_6 octahedron along the local [111] direction, i.e., the z-axis of the hexagonal lattice), the t_{2g} splits further into a lower e'_g doublet and a higher a_{1g} singlet. The trigonal prismatic coordination produces the Ni 3d crystal-field level sequence (from low to high) as $3z^2 - r^2$/xy, $x^2 - y^2$/xz, yz.

along the [111] direction of the local IrO_6 octahedra. Moreover, the e'_g doublet can be expressed as $\sqrt{2/3}xy + \sqrt{1/3}yz$ and $\sqrt{2/3}(x^2 - y^2) - \sqrt{1/3}xz$, when the y-axis is set along the $[1\bar{1}0]$ direction of the local IrO_6 octahedra (then the x-axis is uniquely defined and the xy is in the hexagonal ab plane). By integrating the DOS and determining the center of gravity for each eigen orbital within the antibonding energy range, we find that the e'_g doublet is lower than the a_{1g} singlet by 0.21 eV. Actually, the a_{1g}-e'_g level splitting is an important issue. The trigonal distortion of the IrO_6 octahedron[19], e'_g-e_g mixing[32], and long-ranged crystal field due to the lattice anisotropy[33] all contribute to the splitting. All these effects are properly included in the LDA calculation. Although the contribution of the lattice anisotropy is often quite complicate[33], the a_{1g}-e'_g level ordering can be understood, as the elongation of the IrO_6 octahedron along the [111] direction (the resultant O-Ir-O bond angle deviating from the ideal 90° by 5.4°[28]) raises a_{1g} with respect to e'_g, and the e'_g-e_g mixing pushes e'_g downwards[32]. For the Ni ion, its trigonal prismatic coordination produces the crystal-field level sequence of the Ni 3d electrons as $3z^2 - r^2$/ xy, $x^2 - y^2$/xz, yz (0/0.57/0.76 eV). Furthermore, there are inter-site interactions between the Ir 5d and Ni 3d orbitals, see Fig. 2. The Ir a_{1g} $3z^2 - r^2$and Ni $3z^2 - r^2$ electrons have a lobe pointing to each other and have a ddσ hybridization. The Ir e'_g orbital has, via it's xz or yz component, a ddπ hybridization with the Ni xz/yz; and via it's xy or $x^2 - y^2$ component, a weak ddδ hybridization with the Ni xy/$x^2 - y^2$. Note that those crystal-field level sequences and the Ir-Ni inter-orbital hybridizations are crucial for understanding of the spin-orbital state and the intrachain magnetism in Sr_3MIrO_6, as seen below.

Spin polarization and electron correlation. Then we perform spin-polarized LSDA calculations. We start with a FM or an AF state with the Ni^{2+} spin = 1 and Ir^{4+} spin = 1/2, but both calculations converge to a same FM metallic solution (not shown here). It has a total spin moment of 2.82 μ_B/fu, consisting of the local spin moments of 1.46 μ_B/Ni^{2+}, 0.54 μ_B/Ir^{4+}, and 0.11 μ_B/O. The Ni^{2+} ion has the electronic configuration $(3z^2-r^2)^2(xy,x^2-y^2)^4(xz,yz)^2_\uparrow$, and the Ir^{4+} has a single t_{2g} hole mostly on the a_{1g} orbital [i.e., $(e'_g)^4 a^1_{1g\uparrow}$]. The Ir-O and Ni-O covalencies bring about an appreciable spin moment of 0.11 μ_B on each oxygen. As the a_{1g} orbital is a higher crystal-field level than the e'_g, the a_{1g} hole state allows a direct a_{1g} electron hopping from Ni^{2+} to Ir^{4+}, and this prompts the FM metallic solution.

The above LSDA metallic solution contradicts the experimental insulating behavior. In order to probe the electron correlation effect, we now carry out LSDA + U calculations. The electron correlation stabilizes the Ni^{2+} S = 1 state and the calculated spin moment of Ni^{2+} is enhanced to 1.68 μ_B. As seen in Fig. 3(a), the single Ir^{4+} t_{2g} hole now fully occupies the down-spin a_{1g} orbital. The Ir^{4+} spin moment is also increased to 0.64 μ_B. Owing to the correlation driven d-electron localization, the induced 2p spin moment on oxygen via the Ir-O and Ni-O hybridizations is reduced to 0.08 μ_B. Apparently, electron correlations make the Ir 5d and Ni 3d spin-orbital states fully polarized, thus giving an insulating solution. The tiny band gap is within the Ir t_{2g} shell, and it is due to a relatively weak electron correlation of delocalized 5d electrons. As Ir^{4+} has the single t_{2g} hole on the down-spin a_{1g} ($3z^2 - r^2$) orbital, the down-spin $3z^2 - r^2$ electron of Ni^{2+} can hop forth and back. In order to maximize the local Hund exchange on the virtual Ni^{3+} ion in the excited intermediate state, the hopping $3z^2 - r^2$ electron should be in the minority-spin channel, see Fig. 4 (b). Then this exchange mechanism gives the FM coupling between Ir^{4+} S = 1/2 and Ni^{2+} S = 1. Indeed, our LSDA + U calculation gives a total maximal spin moment of 3 μ_B/fu for this FM insulating state. Here we note that the Ir^{4+} a_{1g} ($3z^2 - r^2$) orbital is orthogonal to the Ni^{2+} xz/yz and xy/$x^2 - y^2$ orbitals, and hence there is no hopping between them to account for the magnetism. Moreover, the Ir^{4+} e_g

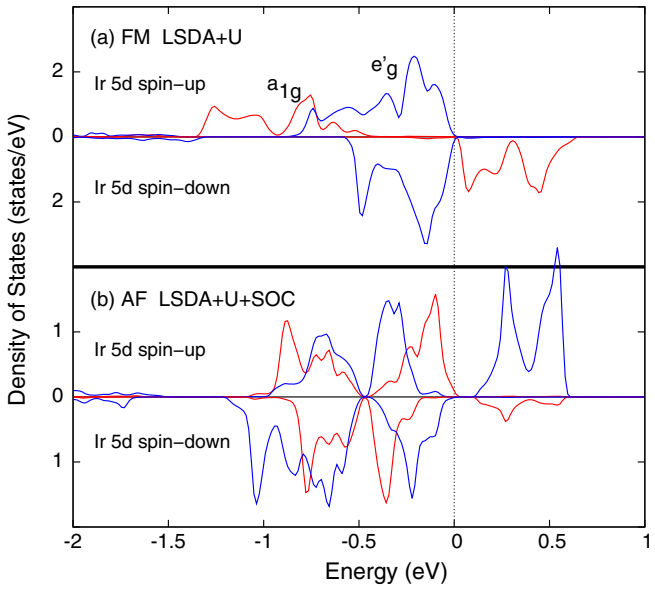

Figure 3 | The partial DOS of the Ir-5d a_{1g} and e'_g orbitals in Sr_3NiIrO_6 in (a) the FM state calculated by LSDA + U and in (b) the AF state by LSDA + U + SOC. Taking the Ni^{2+} S = 1 as a reference, the Ir^{4+} ion has a down-spin a_{1g} empty state in (a) but an up-spin e'_g empty state (i.e., a complex orbital with $l_z = 1$) in (b).

empty bands are too high (see Fig. 2) to be relevant for the magnetic coupling. Therefore, with the crystal-field level diagrams depicted in Figs. 4(a) and 4(b), the electron correlation and inter-orbital hybridization give rise to the FM insulating solution.

Spin-orbit coupling. As 5d transition metals have an intrinsic strong SOC and particularly iridates are a representative example in this respect, now we are motivated to study the SOC effect by doing LSDA + U + SOC calculations. It is interesting to note that now we get an AF insulating solution with a small band gap of 0.15 eV, see Fig. 3(b). Particularly, this solution has the Ir^{4+} single t_{2g} hole on the e'_g orbital, in sharp contrast to the a_{1g} hole state in the above LSDA + U FM insulating solution. The Ni^{2+} retains its configuration state and has a spin moment of 1.69 μ_B. Owing to the small crystal-field splitting of 0.19 eV between (xy, $x^2 - y^2$) and (xz,yz), a finite mixing between them due to the Ni SOC gives also a small orbital moment of 0.21 μ_B on Ni^{2+}. The Ir^{4+} ion has now a spin moment of −0.44 μ_B. Moreover, the e'_g doublet can form a complex orbital with $l_z = \pm 1$.

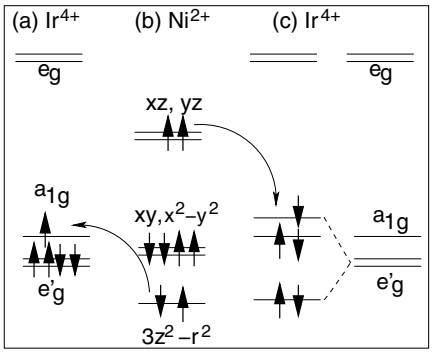

Figure 4 | Schematic level diagrams of the Ir^{4+} 5d and Ni^{2+} 3d orbitals. The down-spin $3z^2 - r^2$ electron mediates a FM coupling via a ddσ hybridization [(a) and (b)]. The up-spin xz/yz electrons mediate an AF coupling via a ddπ hybridization [(b) and (c)], in which the SOC splits the e'_g doublet.

Then in the up-spin channel, the SOC lowers $l_z = -1$ state, and the $l_z = 1$ state is pushed above the Fermi level by SOC and moderate electron correlation, determining the modest band gap and giving an orbital moment of −0.51 μ_B on Ir^{4+}. Owing to the significant Ir-O covalency, both the spin and orbital moments are reduced from their respective ideal unit value. In the AF state of Ni^{2+} S = 1 and Ir^{4+} S = −1/2, the induced magnetic moment on oxygen gets tiny (only about 0.01 μ_B).

Discussion

The above results indicate an interesting evolution of the intrachain magnetic structure, from the LSDA + U FM state to the LSDA + U + SOC AF state. It is ascribed to the SOC tuning orbital state of the Ir^{4+} ion. Although the a_{1g} is a higher crystal-field level than the e'_g by 0.21eV, the significant SOC of the Ir^{4+} ion (being about 0.5 eV) can well split the e'_g doublet and eventually places the upper branch above the a_{1g} (Fig. 4(c)). As a result, the single t_{2g} hole of the Ir^{4+} ion lies in the e'_g state. Then, the up-spin xz/yz electrons of the Ni^{2+} ion can hop, forth and back, to the up-spin e'_g empty state (i.e., the up-spin $l_z = 1$ branch), giving rise to the AF coupling via the ddπ hybridization (Figs. 4(b) and 4(c)). Actually, using the orbital states depicted in Figs. 4(b) and 4(c), we also calculated the FM state. Our LSDA + U + SOC calculations find that the FM state is indeed less stable than the AF ground state by 67 meV/fu. Corresponding LSDA + U + SOC calculations, with Hund exchange parameter J = 0.9 eV for Ni 3d and J = 0.4 eV for Ir 5d, find that the AF ground state is more stable than the FM state by 63 meV/fu. In addition, the spin (orbital) magnetic moment changes within 0.1 (0.05) μ_B. Therefore, here the J parameter has an insignificant influence on the calculated results. As the SOC is intrinsic in iridates, the AF ground state is deemed reliable from the LSDA + U + SOC calculations, but the FM state seems fictitious from the LSDA + U calculations without inclusion of the SOC. Indeed, the AF ground state agrees with the most recent experiment[30]. Therefore, we can conclude that it is the significant SOC of the Ir^{4+} ion which tunes the spin-orbital states and Ir-Ni inter-orbital interactions and hence determines the AF structure of Sr_3NiIrO_6.

Now we turn to Sr_3CoIrO_6. As this material has practically the same crystal structure as Sr_3NiIrO_6[28,30], both systems have many common features in the electronic and magnetic structures. The a_{1g} singlet of the Ir^{4+} ion is higher than the e'_g doublet in the crystal-field level diagram. Moreover, the high-spin Co^{2+} ion has the same crystal-field level sequence as Ni^{2+}, but it now has one hole on the xy/$x^2 - y^2$ doublet (compared with Ni^{2+}, see Fig. 4(b)). Our LSDA + U calculations give a FM metallic solution due to the $3z^2 - r^2$ electron hopping and the 3/4 filled xy/$x^2 - y^2$ bands. Apparently, this solution contradicts the experimental AF insulating behavior[30].

However, when we include SOC by doing LSDA + U + SOC calculations, we have obtained the correct AF insulating solution (see Fig. 5) in good agreement with the experiment[30]. The high-spin Co^{2+} ion (S = 3/2) has a spin moment of 2.66 μ_B. In its down-spin channel, the xy/$x^2 - y^2$ doublet form the complex orbitals ($x^2 - y^2$) ± ixy with $l_z = \pm 2$, and the Co^{2+} SOC lowers the $l_z = 2$ state but lifts the $l_z = -2$ state. The electron correlation places the former at −1.5 eV and the latter at 2 eV. As a result, the Co^{2+} ion has also a huge orbital moment of 1.71 μ_B. In total, the Co^{2+} ion has the magnetic moment of 4.37 μ_B and it is firmly aligned, due to the SOC, along the hexagonal c-axis (i.e., a significant Ising-like spin system). Moreover, the Ir 5d states are almost the same as in Sr_3NiIrO_6: the Ir^{4+} SOC places the single t_{2g} hole on the e'_g doublet; the SOC and moderate electron correlation determine the small insulating gap within the Ir^{4+} t_{2g} shell, see Fig. 5. The Ir^{4+} ion has the spin (orbital) moment of −0.39 (−0.47) μ_B and in total −0.86 μ_B. Using these spin-orbital states, our LSDA + U + SOC calculations find that the AF ground state is more stable than the FM state by 122 meV/fu, which changes

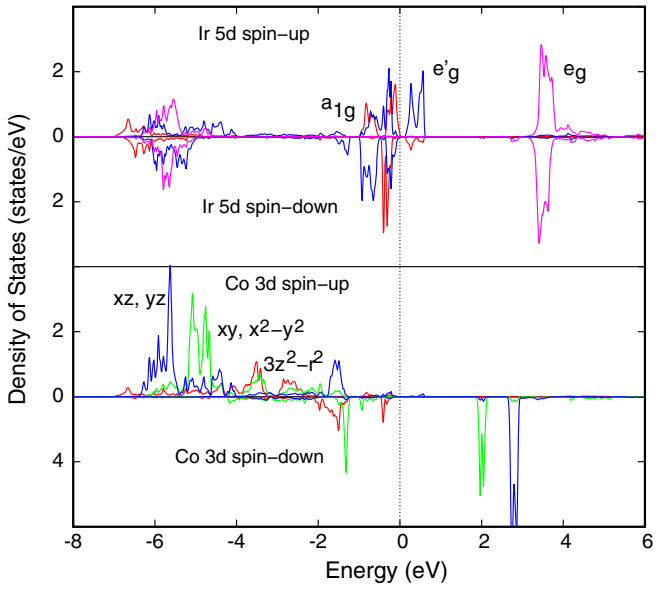

Figure 5 | The partial DOS of the Ir 5d and Co 3d eigen orbitals in AF Sr_3CoIrO_6 calculated by LSDA + U + SOC. The high-spin Co^{2+} ion (S = 3/2) has the orbitals $3z^2 - r^2$ (red curve) and $\left[(x^2-y^2)+ixy\right]/\sqrt{2}$ ($l_z=2$) occupied (green curve) in its down-spin channel. The Ir^{4+} (S = −1/2) has the e_g' $l_z = 1$ empty state (blue curve) in its up-spin channel.

little to 130 meV/fu when including Hund exchange J = 0.9 eV for Co 3d and J = 0.4 eV for Ir 5d.

By looking at Figs. 4(b) and 4(c), and now having also one hole on the down-spin xy/$x^2 - y^2$ doublet for Co^{2+}, we find that the net spin = 1 from xz/yz and the net spin = 1/2 from xy/$x^2 - y^2$ both contribute to the AF exchange with the net Ir spin = −1/2 from the e_g'. The former is via a ddπ hybridization as in Sr_3NiIrO_6, and the latter a weaker ddδ one (which is missing in Sr_3NiIrO_6). This, together with the spin values (Co^{2+} S = 3/2 vs Ni^{2+} S = 1), qualitatively accounts for a higher stability of the AF ground state over the FM state in Sr_3CoIrO_6 than in Sr_3NiIrO_6, i.e., 122 vs 67 meV/fu. In addition, the ddδ hybridization results in the smaller spin and orbital moments of the Ir^{4+} ion in Sr_3CoIrO_6 (0.39 + 0.47 μ_B) than in Sr_3NiIrO_6 (0.44 + 0.51 μ_B). Note that all these results qualitatively explain the (slightly) higher intrachain AF transition temperature of 90 K in Sr_3CoIrO_6 than 85 K in Sr_3NiIrO_6[30]. Moreover, the calculated magnetic moments of the significant Ising type, 4.37 μ_B/Co^{2+} and −0.86 μ_B/Ir^{4+}, also agree reasonably well with the experimental ones of 3.6 and −0.6 μB in Sr_3CoIrO_6[30].

In summary, using density functional calculations including spin-orbit coupling (SOC) and electron correlation, we have demonstrated that the SOC of the Ir^{4+} ion plays an essential role in determining the antiferromagnetism of the hexagonal spin-chain system Sr_3MIrO_6 (M = Ni, Co) by tuning the crystal-field level sequence and altering the Ir-M inter-orbital interactions. The SOC splits the e_g' doublet of the octahedral Ir^{4+} ion (t_{2g}^5) in a trigonal crystal field, and the single t_{2g} hole resides on the e_g' upper branch and gives rise to the antiferromagnetic superexchange. In absence of the SOC, however, the single t_{2g} hole would occupy the a_{1g} singlet instead, which would mediate an unreal ferromagnetic exchange due to a direct a_{1g} hopping along the Ir-M chain. We also find that the Ni^{2+} and Co^{2+} ions are both in a high-spin state and moreover the Co^{2+} ion carries a huge orbital moment. This work well accounts for the most recent experiments and magnifies again the significance of the SOC in iridates.

Methods

We have carried out density functional calculations, using the full-potential augmented plane wave plus local orbital code (Wien2k)[34]. We use the structural data of Sr_3NiIrO_6 measured by neutron diffraction at 10 K[28] and of Sr_3CoIrO_6 at 4 K[30]. They have practically the same crystal structure: the Ir-O bondlength of 2.01 Å, the M-O 2.18 Å, and the M-Ir 2.78 Å for M = Ni and Co; the small deviation of the O-Ir-O bond angle (from the ideal 90°) due to a small elongated trigonal distortion of the IrO_6 octahedron, being 5.4° for M = Ni and 5.2° for M = Co. The muffin-tin sphere radii are chosen to be 2.8, 2.2, 2.2 and 1.5 Bohr for Sr, Ni/Co, and Ir and O atoms, respectively. The plane-wave cut-off energy of 16 Ry is set for the interstitial wave functions, and 5 × 5 × 5 **k** mesh for integration over the rhombohedral Brillouin zone. Using 7 × 7 × 7 **k** mesh (more than a doubling) gives practically the same results, with the total energy converging within 2 meV/fu. We employ the local spin density approximation[35] plus Hubbard U (LSDA + U) method[36] to describe the electron correlation of the M 3d and Ir 5d electrons, with the LSDA + U double counting correction made in a fully atomic limit[36]. The typical values, effective U = 2, 4 and 5 eV (U_{eff} = U − J with Hund exchange parameter J being set at zero) are used for the Ir 5d, Co 3d, and Ni 3d states, respectively. Note that our key results –the coupled spin-orbital state and the magnetic ground state –are independent of the tested U values (1–3 eV for Ir 5d and 3–7 eV for Co/Ni 3d). To account for (near) degeneracy of the Ir 5d orbitals (and of M 3d orbitals as well), the SOC is included by the second-variational method with scalar relativistic wave functions. In order to probe diverse possible spin-orbital states and magnetic structures, we excess them in our calculations by setting their respective occupation number matrix and thus orbitally dependent potentials, and then do self-consistent calculations including a full electronic relaxation. (Otherwise, some states of the concern or even the ground state cannot be achieved.) An advantage of this procedure is such that we can reliably determine the magnetic ground state by a direct comparison of the different states[19,21].

1. Dagotto, E. Complexity in strongly correlated electronic systems. *Science* **309**, 257–262 (2005).
2. Kim, B. *et al.* Novel J_{eff} = 1/2 Mott State Induced by Relativistic Spin-Orbit Coupling in Sr_2IrO_4. *Phys. Rev. Lett.* **101**, 076402 (2008).
3. Kim, B. J. *et al.* Phase-sensitive observation of a spin-orbital Mott state in Sr_2IrO_4. *Science* **323**, 1329–1332 (2009).
4. Shitade, A. *et al.* Quantum Spin Hall Effect in a Transition Metal Oxide Na_2IrO_3. *Phys. Rev. Lett.* **102**, 256403 (2009).
5. Pesin, D. & Balents, L. Mott physics and band topology in materials with strong spin–orbit interaction. *Nat. Phys.* **6**, 376–381 (2010).
6. Wang, F. & Senthil, T. Twisted Hubbard Model for Sr_2IrO_4: Magnetism and Possible High Temperature Superconductivity. *Phys. Rev. Lett.* **106**, 136402 (2011).
7. Jackeli, G. & Khaliullin, G. Mott insulators in the strong spin-orbit coupling limit: from Heisenberg to a quantum compass and Kitaev models. *Phys. Rev. Lett.* **102**, 017205 (2009).
8. Chaloupka, J., Jackeli, G. & Khaliullin, G. Kitaev-Heisenberg Model on a Honeycomb Lattice: Possible Exotic Phases in Iridium Oxides A_2IrO_3. *Phys. Rev. Lett.* **105**, 027204 (2010).
9. Wan, X., Turner, A. M., Vishwanath, A. & Savrasov, S. Y. Topological semimetal and Fermi-arc surface states in the electronic structure of pyrochlore iridates. *Phys. Rev. B* **83**, 205101 (2011).
10. Yin, W.-G. *et al.* Ferromagnetic Exchange Anisotropy from Antiferromagnetic Superexchange in the Mixed 3d–5d Transition-Metal Compound Sr_3CuIrO_6. *Phys. Rev. Lett.* **111**, 057202 (2013).
11. Haskel, D. *et al.* Pressure Tuning of the Spin-Orbit Coupled Ground State in Sr_2IrO_4. *Phys. Rev. Lett.* **109**, 027204 (2012).
12. Mazin, I. I., Jeschke, H. O., Foyevtsova, K., Valentí, R. & Khomskii, D. I. Na_2IrO_3 as a Molecular Orbital Crystal. *Phys. Rev. Lett.* **109**, 197201 (2012).
13. Katukuri, V. M., Stoll, H., van den Brink, J. & Hozoi, L. Ab initio determination of excitation energies and magnetic couplings in correlated quasi-two-dimensional iridates. *Phys. Rev. B* **85**, 220402 (2012).
14. Gretarsson, H. *et al.* Crystal-Field Splitting and Correlation Effect on the Electronic Structure of A_2IrO_3. *Phys. Rev. Lett.* **110**, 076402 (2013).
15. Li, Q. *et al.* Atomically resolved spectroscopic study of Sr_2IrO_4: experiment and theory. *Sci. Rep.* **3**, 3073 (2013).
16. Cao, G. *et al.* Magnetism and electronic structure of La_2ZnIrO_6 and La_2MgIrO_6: Candidate J_{eff} = 1/2 Mott insulators. *Phys. Rev. B* **87**, 155136 (2013).
17. Ou, X. & Wu, H. Coupled charge-spin-orbital state in Fe-or Co-doped Sr_2IrO_4. *Phys. Rev. B* **89**, 035138 (2014).
18. Niitaka, S., Yoshimura, K., Kosuge, K., Nishi, M. & Kakurai, K. Partially Disordered Antiferromagnetic Phase in Ca_3CoRhO_6. *Phys. Rev. Lett.* **87**, 177202 (2001).
19. Wu, H., Haverkort, M. W., Hu, Z., Khomskii, D. I. & Tjeng, L. H. Nature of Magnetism in $Ca_3Co_2O_6$. *Phys. Rev. Lett.* **95**, 186401 (2005).
20. Choi, Y. J. *et al.* Ferroelectricity in an Ising Chain Magnet. *Phys. Rev. Lett.* **100**, 047601 (2008).
21. Wu, H. *et al.* Ising Magnetism and Ferroelectricity in Ca_3CoMnO_6. *Phys. Rev. Lett.* **102**, 026404 (2009).
22. Agrestini, S. *et al.* Slow Magnetic Order-Order Transition in the Spin Chain Antiferromagnet $Ca_3Co_2O_6$. *Phys. Rev. Lett.* **106**, 197204 (2011).

23. Kamiya, Y. & Batista, C. D. Formation of Magnetic Microphases in $Ca_3Co_2O_6$. *Phys. Rev. Lett.* **109**, 067204 (2012).
24. Whangbo, M.-H., Dai, D., Koo, H.-J. & Jobic, S. Investigations of the oxidation states and spin distributions in $Ca_3Co_2O_6$ and Ca_3CoRhO_6 by spin-polarized electronic band structure calculations. *Solid State Commun.* **125**, 413–417 (2003).
25. Eyert, V., Laschinger, C., Kopp, T. & Frésard, R. Extended moment formation and magnetic ordering in the trigonal chain compound $Ca_3Co_2O_6$. *Chem. Phys. Lett.* **385**, 249–254 (2004).
26. Vidya, R., Ravindran, P., Fjellvag, H., Kjekshus, A. & Eriksson, O. Tailor-made electronic and magnetic properties in one-dimensional pure and Y-substituted $Ca_3Co_2O_6$. *Phys. Rev. Lett.* **91**, 186404 (2003).
27. Frésard, R., Laschinger, C., Kopp, T. & Eyert, V. Origin of magnetic interactions in $Ca_3Co_2O_6$. *Phys. Rev. B* **69**, 140405(R) (2004).
28. Nguyen, T. & Zur Loye, H.-C. A Family of One-Dimensional Oxides: Sr_3MlrO_6 (M = Ni, Cu, Zn): Structure and Magnetic Properties. *J. Solid State Chem.* **117**, 300–308 (1995).
29. Sarkar, S., Kanungo, S. & Saha-Dasgupta, T. Ab initio study of low-dimensional quantum spin systems Sr_3NiPtO_6, Sr_3CuPtO_6, and Sr_3NiIrO_6. *Phys. Rev. B* **82**, 23122 (2010).
30. Mikhailova, D. *et al.* Magnetic properties and crystal structure of Sr_3CoIrO_6 and Sr_3NiIrO_6. *Phys. Rev. B* **86**, 13409 (2012).
31. Zhang, G. R., Zhang, X. L., Jia, T., Zeng, Z. & Lin, H. Q. Intrachain antiferromagnetic interaction and Mott state induced by spin-orbit coupling in Sr_3NiIrO_6. *J. Appl. Phys.* **107**, 09E120 (2010).
32. Landron, S. & Lepetit, M.-B. Importance of t_{2g}-e_g hybridization in transition metal oxides. *Phys. Rev. B* **77**, 125106 (2008).
33. Wu, H. *et al.* Orbital order in $La_{0.5}Sr_{1.5}MnO_4$: Beyond a common local Jahn-Teller picture. *Phys. Rev. B* **84**, 155126 (2011).
34. Blaha, P., Schwarz, K., Madsen, G., Kvasnicka, D. & Luitz, J. *WIEN2k: An augmented plane wave plus local orbitals program for calculating crystal properties, Vienna University of Technology, Austria* (2001).
35. Perdew, J. P. & Wang, Y. Accurate and simple analytic representation of the electron-gas correlation energy. *Phys. Rev. B* **45**, 13244–13249 (1992).
36. Anisimov, V. I., Solovyev, I. V., Korotin, M. A., Czyżyk, M. T. & Sawatzky, G. A. Density-functional theory and NiO photoemission spectra. *Phys. Rev. B* **48**, 16929–16934 (1993).

Acknowledgments

This work was supported by the NSF of China (Grant No. 11274070), PuJiang Program of Shanghai (Grant No. 12PJ1401000), and ShuGuang Program of Shanghai (Grant No. 12SG06). X.O. was also supported by the Outstanding Doctoral Student Project of Fudan University.

Author contributions

H.W. conceived the idea and designed the research. X.O. and H.W. performed the calculations. H.W. and X.O. prepared the manuscript.

Additional information

Competing financial interests: The authors declare no competing financial interests.

How to cite this article: Ou, X. & Wu, H. Impact of spin-orbit coupling on the magnetism of Sr_3MIrO_6 (M = Ni, Co). *Sci. Rep.* **4**, 4609; DOI:10.1038/srep04609 (2014).